Risk based portfolio planning of dike reinforcements

den Heijer, Frank; Kok, Matthijs

DOI
10.1016/j.ress.2023.109737

Publication date
2023

Document Version
Final published version

Published in
Reliability Engineering and System Safety

Reliability Engineering and System Safety 242 (2024) 109737

Contents lists available at ScienceDirect

Reliability Engineering and System Safety

journal homepage: www.elsevier.com/locate/ress

Risk-based portfolio planning of dike reinforcements

Frank den Heijer [a,*], Matthijs Kok [b]

[a] HAN University of Applied Sciences, Ruitenberglaan 26 Arnhem, CC 6826, The Netherlands
[b] Delft University of Technology, Stevinweg 1 Delft, CN 2628, The Netherlands

ARTICLE INFO

Keywords:
Flood risk
Tactical decision making
Portfolio planning
Dike reinforcements

ABSTRACT

A system of dikes in flood-prone areas continuously requires measures to mitigate changes such as ageing and climate change. Planning costly measures requires proper insight into system risk effects. Especially in a riverine dike system, the risk contributions of individual assets to the system flood risks are not independent, because reinforcement of a dike upstream increases the risks downstream. Tactical plans define the planning of consecutive measures to implement a flood risk reduction strategy, which may take decades. They may differ due to choices such as a prioritization metric, planning conditions and budget. In this study, a method is developed to compare different tactics to prioritize and plan measures in interdependent systems of dikes to reduce risks most effectively and efficiently. A case study meant as a proof of concept was carried out for the reinforcement of about 500 km of dikes along the Rhine River branches in the Netherlands. We studied the effects of 12 different tactical plans on the aggregated risks over time. The economic risks differ by up to about 40%, and the risks on victims differ by up to 70 %. We conclude that tactical planning and corresponding decisions are important for reduction of time-aggregated flood risks.

1. Introduction

Deltaic areas are often protected against flooding by defence systems of dikes, dunes and hydraulic structures near the sea, and more upstream mostly by systems of dikes. The probability of flooding times the negative consequences like victims and economic damage are referred to as flood risks. Flood defences are ageing, due to subsidence or deterioration of revetment material. As well, the performance of flood defences decreases due to the increase of loads caused by climate change. Therefore, as long as the area has to be protected against flooding, interventions are required in the flood defence system to mitigate increasing risks.

Management of large portfolios of dikes consists of several decision levels [26,63], based on the ISO 55,000 series. Operational management contains aspects such as regular inspections, maintenance and reinforcements [32], in the taxonomy of maintenance strategies described by Carpitella et al. [8] referred to as condition-based or predictive maintenance. Strategic management contains aspects such as how to prepare for uncertain climate change, and the development of safety standards and long-term spatial developments [29,42,47]. Tactic management connects strategic and operational management [63], containing aspects such as prioritization and planning of reinforcements in the system. The planning of reinforcements and other interventions takes place within the boundaries given by the flood risk strategy. Following the terminology in [63] and [39] we use 'tactical' asset management in this paper to prevent confusion with strategic asset management. When a strategy is a plan in outline to achieve a goal, a tactic is a way to implement the strategy to achieve that goal.

The main objective of proper asset management is to balance risks, performance and cost over time, to align asset-related spending to institutional goals [6,20,39]. A dike system is not in balance in case of sudden changes such as the adoption of more stringent safety standards or new knowledge. Dike reinforcements may be required in the whole system to become compliant. This is also the case when new climate projections or new spatial development goals are adopted. The corresponding efforts are large relative to planning issues for a system in balance. Since budgets, outsourcing and contractors' execution capacity are limited, it will take time to become compliant and restore a balanced system. In Fig. 1 this is schematically presented. We define the portfolio risk as the total risk in the system, and the risk deficit as the surface between the actual portfolio risk in time and the compliant risk level, which is the portfolio risk in case all dikes in the system are exactly compliant. The larger the risk deficit relative to executing capacity, the longer the period the system does not satisfy the pursued compliant risk level.

* Corresponding author.
E-mail address: frank.denheijer@han.nl (F. den Heijer).

https://doi.org/10.1016/j.ress.2023.109737
Received 5 April 2023; Received in revised form 11 September 2023; Accepted 12 October 2023
Available online 18 October 2023

A tactical plan leads to a programme of interventions in a portfolio. Different tactical plans lead to different intervention schemes. In Fig. 2 a programme is schematically presented. It propagates in time, changing each timeframe due to realisation, new, postponed or withdrawn projects.

Especially in a riverine dike system, the risk contributions of individual assets to the flood risk in the system are not independent [10,16]. Reinforcement of a dike upstream increases the risks downstream. In the classification of infrastructure interdependencies in Sharma, Nocera, and Gardoni [49] a riverine dike system could be best described as episodic (dependency only during floods and dike breaches). Thus, a dike reinforcement upstream reducing a small risk, may even increase the total system risk. Therefore, the relation between the individual asset risk contributions and system risks is very non-linear. This specifically leads to continuous changing contributions of individual assets risks to system risks, depending on the measures executed in time and space.

Therefore, to reduce system risks in time the order and planning of reinforcements matters. In this article, we present a method to compare the aggregated risks over time of tactical plans to prioritize and plan compliance measures, and an application for a portfolio of dikes in a riverine system. The novel contribution to literature is the physics-based dependence-modelling for the tactical intervention management over time. To focus on the effect of tactical asset management decisions, this study is based on a single flood risk strategy to pursue compliance with standards by dike reinforcements.

We consecutively present the theoretical background of planning flood risk systems, the development of a risk-based method for prioritization and planning of a system of dikes and the metrics to enable comparison, and a case study meant as a proof of concept, which was carried out for the dikes along the Rhine River branches which is planned to last for decades. We close with the discussion and conclusions.

2. Literature overview

Meteo and water systems cause loads along flood defences systems, and consequences could affect a large area. Derivation of maintenance policies for a portfolio of degrading assets under climate change with budget constraints, needs thorough system analyses [43,44,66].

Quantitative risk-based system approaches have been widely adopted in the practice of flood defence management. In [57] an optimal flood defence system safety level is derived for a large polder in the Netherlands based on the economic risk. Based hereon the Dutch safety standards have been established [12] for other polders, also referred to as the criteria determining soft failure [66]. The present Dutch safety standards were re-established in 2017 based on an enhanced economic [17,18] and technical approach [29], based on probabilities of failure for dike overtopping. An extensive risk analysis has been performed taking all failure mechanisms into account [61]. In [46] and [45] the source-pathway-receptor framework is proposed to systematically assess risks. In [56] a conceptual approach is developed and applied to quantify the effects of river system behaviour on probabilities of dike breach and flood risk, for a reduced set of failure mechanisms, concluding that for proper flood risk assessment all relevant dike failure mechanisms, uncertainties as well as all proposed safety improvement measures are to be jointly taken into account. Vorogushyn [64] developed and applied probabilistic flood hazard maps, taking dike breaches in a river branch into account, and considering three failure mechanisms. Domeneghetti, Vorogushyn, Castellarin, Merz, and Brath [14] improved the approach adding the effect of uncertain boundary conditions. Bachmann [3] developed a risk-based model for decision support on measures on the scale of a catchment area. Bachmann and Schüttrumpf [5] took into account the effect of dike breaches in the system and Curran [11] improved the hydrological modelling of dependencies in the river branches and cascade effects of polders. The presented system risk analyses all refer to the actual status of the flood defences to consider the risks and effects of potential measures.

In [63] the poor interconnection between strategic and operational flood defence asset management is addressed, emphasizing the need to strengthen the interconnecting tactical handshake to better factor deterioration into planning. In Dupuits et al. [16] a time-dependant economic flood risk optimization is performed to determine the optimal development of safety standards in the long term in a small interdependent river system, however, without planning constraints such as budget. Klerk, Kanning, Kok, and Wolfert [31] elaborated on the cost-optimal prioritization of interventions for the reinforcement of non-homogeneous segments of dikes. They showed the considerable effect of intervention tactics on Life Cycle Costs (LCC). However, they focused on prioritization, simplified the risk analysis and did not study the planning of measures in time.

Prioritization and planning of costly measures in large infrastructure systems requires proper insight into system risk effects (Liu, 2023). It requires to look forward to uncertain circumstances at the design horizon. Buijs, Hall, Sayers, and Van Gelder [7] performed time-dependant reliability analysis for flood defences in the Thames estuary and Roubos, Allaix, Schweckendiek, Steenbergen, and Jonkman [40] did so for corrosion analyses of quay walls. Mens [35] researched the system robustness of one of the branches of the Rhine River, comparing system risks for different strategies. Haasnoot, Kwakkel, Walker, and Ter Maat [22] developed a qualitative approach for decision-making under deep uncertainty called ‘Dynamic Adaptive Policy Pathways’ (DAPP). They introduced the opportunity to consider different perspectives to choose a robust strategy. Manocha and Babovic [34] and Toimil, Losada, Hinkel, and Nicholls [54] added quantitative elements to DAPP for the management of storm water infrastructure and coastal erosion. The DAPP

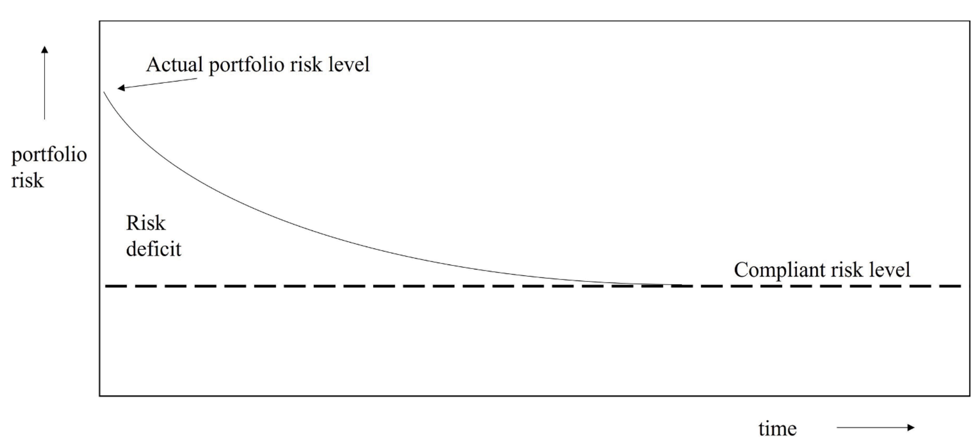

Fig. 1. Schematic representation of actual portfolio risk level and risk deficit in time in case measures are effective.

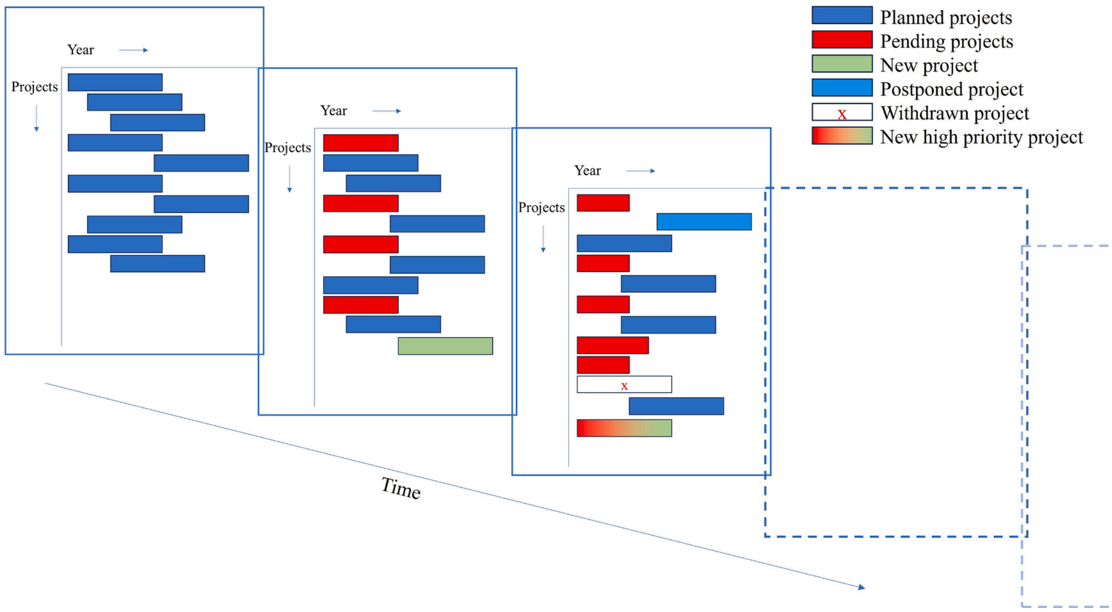

Fig. 2. Schematic representation of a programme window with projects (vertical axis) and planning (horizontal axis) propagating in time.

approach does not provide intervention planning, and requires discrete chosen scenarios and strategies.

In research on related water infrastructure, the tactical interconnection based on time-dependant risk analyses is increasingly addressed to prioritize measures. Young and Hall [70] performed a systems perspective on investments in the Thames Estuary region, including infrastructure asset interactions. Smet [52] developed a proactive planning approach for water resource infrastructure investments taking into account uncertain external drivers like climate change as well as uncertain structure-specific drivers like deterioration. Van den Boomen [58] focused on the optimal timing of replacements of public infrastructures with respect to life cycle costs, taking price uncertainty into account. Both focus on individual and independent hydraulic structures rather than systems of assets. Yang and Frangopol [69] developed a robust risk-based single-objective optimisation approach to portfolio management under deep uncertainties, for a set of individual and independent assets like bridges. The method uses proxies for loads, climate change and deterioration in time and allows one intervention per asset. Fluixá-Sanmartín, Escuder-Bueno, Morales-Torres, and Castillo-Rodríguez [19] propose an approach for dam risk management in the long term that considers the time-dependant evolution of risk, ranking the priority of present measures to optimally reduce dam risks. Liu, Tang, D. Huang, Z. Huang, Zhang and Xu [33] presents a probabilistic measure for the potential risk of regional roads exposed to landslides, providing guidance for spatial and hierarchical risk management.

Systems with many components in different states are elaborated extensively with mathematical models, e.g. in [38,68], e.g. using fault tree analysis, failure mode analysis, bow-tie analysis, and Markov models. In these approaches it is important to find solutions reducing the explosive number of samples in reliability analyses. Model-based approaches gain increasing attention [24]. Especially when cascading effects may occur [37], or in case of integrated reliability analysis, remaining useful life analyses and maintenance actions [71], the model based approaches support reducing the explosive number of combinations of state and space [21].

To summarise, much work has been done on flood risk analysis, system analysis, strategies for the long term, adaptive strategies to cope with climate change, and prioritisation. The modelling of the systems is increasingly improved with respect to scale, failure mechanisms, and mathematic-computational methods. Prioritisation of interventions is done more and more risk-based. However, no work has been found on time-dependant risk-based medium-term planning of interventions in an interdependent, deteriorating system of dikes under climate change. This figures out a clear knowledge gap for flood risk analyses: how to plan interventions in time in a changing system, in which the performance of assets affects the performance of other assets in the same system, as is the case for a system of dikes in a riverine area. In this paper, as especially the physical system dependency affects flood risks, we used a physical-model-based approach to assess space-dependency applied in an integrated system risk analysis and reinforcement planning approach.

3. Methodology

In [69] the portfolio risk is given as the sum of all risks per asset per year, which assets are independent of the performance of others:

$$R_p(t_L) = \sum_{i=1}^{t_L} \sum_{k=1}^{K} R(k,i) = \sum_{i=1}^{t_L} \sum_{k=1}^{K} P_k(i) \cdot d_k(i) \tag{1}$$

In which:

$R_p(t_L)$	The portfolio risk from present to year t_L	€/*year*, *victims*/*year*
i	indicator of year	–
t_L	The time horizon of interest	year
k	indicator of asset, in this study dike section	–
K	The number of assets in the portfolio	–
$R(k,i)$	The risk for asset k in year i	€/*year*, *victims*/*year*
$P_k(i)$	Probability of failure of asset k in year i	per year
$d_k(i)$	The consequences due to failure of asset k in year i, index ER for economic risk, SR for social risk on victims	€/*year*, *victims*/*year*

In this paper, the objective is to enable an analysis of portfolio risks in time for a system of dikes. The system state is given by $P_k(i)$: the probabilities of failure of the dikes in the system in year i. Since the system state changes due to interventions, the risks *R(k,i)* of dike breach at dike section k in year i are intertwined with the interventions on other dike sections in the system. Therefore, the methodology consists of two main steps that are followed over a period of time: the determination of portfolio risks in a year given a system state, and the determination of interventions in the system state given the compliance requirements (e.

g. safety standard) and given planning constraints, see Fig. 3. In the following subsections, we firstly elaborate on a system consisting of a single dike section, secondly, we expand to a system of dike sections, and thirdly we determine the interventions based on system states.

3.1. A single dike in the system

The risk for a single dike section k in year *i* is the probability of failure multiplied by consequences $P_{f_k}(i)\cdot d_k(i)$. The water level is the dominant load for flood risk assessments for both the probability of failure and consequences. The probability of failure for dike section k in year i is assessed by integration of the probability density function (pdf) of water level and a fragility curve, see Fig. 4, as increasingly used in flood risk assessments since the '90s as shown by [48]:

$$P_{f_k}(i) = \int_{h_k(i)} f(h_k(i))\cdot p_{f|h_k}(i)\, dh \tag{2}$$

In which:

$P_{f_k}(i)$	The probability of flooding for dike section k in year i	per year
$f(h_k(i))$	The probability density function of water level $h_k(i)$ along dike section k in year i	per year
$h_k(i)$	Water level along dike section k in year i with respect to reference level SWL (Sea Water Level)	$m+$ SWL
$p_{f\|h_k}(i)$	Conditional probability of failure of dike section k during a flood wave with water level $h_k(i)$ in year i	–

The fragility curves reflect the strength of a dike section, expressed as a curve of conditional probabilities of dike failure for given water levels. Thoroughly derived, this curve includes not only the strength of a dike section but also secondary loads such as wave impacts. An advantage of fragility curves is they can be precalculated based on knowledge and detailed models, and are practical to use in probabilistic models [2,65]. This also enables operational flood risk management during flood waves, supporting decision-making in situations under time pressure [4, 67], as policy analysis and planning decisions [55]. For planning issues as addressed in this article, the fragility curve is time-dependant because of subsidence, and subsequently, the pdf of water level is time-dependant due to climate change. Deterioration due to subsidence is modelled as a shift of the entire fragility curve, in Fig. 4 to the left, gradually in time. Reinforcements are modelled as a sudden shift of the entire fragility curve, in Fig. 4 to the right. In fact, herewith only the measure of dike heightening is considered. Thus, the mean value of the fragility curve for dike section k in year t_L is:

$$\mu_{frag_k}(t_L) = \mu_{frag_k}(0) - s_k\cdot t_L + \sum_{i=0}^{i=t_L} \Delta h_k(i) \tag{3}$$

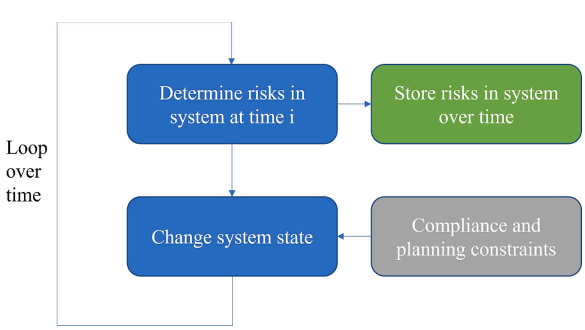

Fig. 3. Schematic overview of methodology to assess the sum of risks over time.

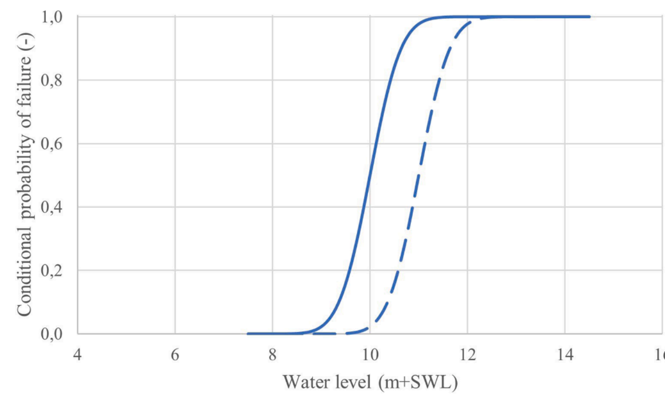

Fig. 4. Example of a fragility curve, here simplified as a normal distribution with a mean of 10m+SWL and a standard deviation of 0.5 m (solid line) and a curve representing a dike heightening of 1 m (dashed line).

In which:

$\mu_{frag_k}(i)$	The mean value of the fragility curve for dike section k in the system in year i	m+SWL
$\mu_{frag_k}(0)$	Mean value or 50% percentile of the fragility curve for dike section k at the start of the analysis, year $i = 0$	m+SWL
s_k	Yearly subsidence for dike section k	m/year
$\Delta h_k(i)$	Increase of mean value of fragility curve due to reinforcement of dike section k in year i	M

We assume that in practice the planning process starts after detailed reliability analysis, delivering the components of Eq. (2): the probability of failure $P_{f_k}(0)$ at the start year of the analysis, the pdf of water level $f(h_k(0))$ and the shape of the fragility curve $P_{f|h_k}(0)$. Therewith, $\mu_{frag_k}(0)$ is known.

The interventions $\Delta h_k(i)$ in time are based on the assessed performances over time. In case the probability in year i rises above the standard and other constraints such as budget are fulfilled a dike reinforcement $\Delta h_k(i)$ is performed. This reinforcement has to be compliant until the design horizon $i+T_{plan}$. Since we know exactly one reinforcement is planned between year i and year $i+T_{plan}$ we can design this reinforcement based on the difference of Eq. (3) between year $i+T_{plan}$ and i:

$$\Delta h_k(i) = s_k\cdot T_{plan} + \left(\mu_{frag_k}(i+T_{plan}) - \mu_{frag_k}(i)\right) \tag{4}$$

In which:

T_{plan}	The design horizon of a reinforcement	*year*

The values for $\mu_{frag_k}(i+T_{plan})$ are derived based on Eq. (2). The probability of failure $P_{f_k}(i+T_{plan})$ is equal to the required standard to be compliant. The pdf of water level $f(h_k(i+T_{plan}))$ is based on a climate change projection. The location $\mu_{frag_k}(i+T_{plan})$ of the fragility curve is solved using the present shape of the fragility curve, which is a reasonable starting point for planning issues since detailed designs are in practice performed as a follow-up. Therewith, the probability of flooding for a single dike section is known in time.

The consequences of failure of a dike section in the system are based on pre-calculated consequences of floodings occurring at different flood characteristics. The economic consequences per year are discounted to the present value. Victims in the future are assumed to be as important as victims nowadays, thus, the 'present value' for victims is a simple sum over the years of interest. Thus, the following equation is used for the risk for a single dike section k in year $_i$:

$$R^{PV}(k,i) = \int_{h_k(i)} f(h_k(i)) \cdot p_{f|h_k}(i) \cdot d(h_k(i)) \cdot \exp(-I_d \cdot r' \cdot i) dh \tag{5}$$

In which:

$R^{PV}(k,i)$	The present value of the flood risk for a single dike section k in year i	€, *victims*
$d(h_k(i))$	Consequences due to a breach in dike section k during a flood wave with water level maximum $h_k(i)$ in year i	€, *victims*
I_d	Indicator for type of consequences (for economic consequences: 1; for victims: 0)	–
r'	Discount rate minus inflation	–

3.2. Multiple dikes in the system

The risk assessment for a portfolio of dikes along a water system is more complex. Firstly, the loads along the dike system depend on a set of water levels, depending on system loads. In river areas, these system loads are mainly river discharges. Near the sea, in estuaries, and in coastal environments they depend also on tides and wind-driven storm surges. Here, these system loads are denoted by $\overrightarrow{S}$. The contribution of a single dike section to the flood risk for the entire system in year i is slightly adapted with respect to Eq. (5) to take into account the effect of system loads on local water levels:

$$R^{PV}(k,i) = \int_{\overrightarrow{S}(i)} f_{\overrightarrow{S}(i)}(h_k) \cdot p_{f|h_k}(i) \cdot d(h_k(i)) \cdot \exp(-I_d \cdot r' \cdot i)\, d\overrightarrow{S}(i) \tag{6}$$

In which:

$\overrightarrow{S}(i)$	System loads, e.g. combination of river discharge and sea water level.	
$f_{\overrightarrow{S}(i)}(h_k)$	The probability density function of system loads in year i, causing local water levels (h_k) at dike sections k.	–

Secondly, the risks of different potential dike breaches interrelate because the water levels along the water system affect each other in case of a failure of one of the stretches. A breach upstream of a river lowers the downstream water levels and thus affects both the probabilities of failure of stretches downstream and their consequences. Therefore, a simple sum of risks per individual dike stretch in Eq. (6) does not hold. In this proof of concept for planning issues, the effect of breach discharges on downstream river water levels is estimated with the spillway formula at critical flow [27,30]:

$$Q_{breach} = C_e \cdot B \cdot \frac{2}{3} \sqrt{2g} \cdot \left(h_k - h_{b_k}\right)^{1.5} \tag{7}$$

In which:

C_e	Spillway discharge coefficient, here assumed to be the minimal value in [30] of $1/\sqrt{3} \approx 0.58$.	–
B	Breach width.	*m*
h_{b_k}	Bottom level at breach location.	*m*

Note, with Eq. (7) we over-estimated the effect of a breach on downstream river water levels because the breach volume is assessed as a suddenly occurring breach with a width B at the event water level maximum, neglecting the backwater effect of polder water levels. Note, we do not use Eq. (7) for the estimation of consequences $d(h_k(i))$ since backwater effects are considered to be important for consequence estimates.

With breach effects the load distribution $f_{\overrightarrow{S}(i)}(h_k)$ is transformed in $f'_{\overrightarrow{S}(i)}(h_k)$. We sum the risks for the whole portfolio of dikes k given an individual load event $\overrightarrow{S}(i)$, taking into account the transformed water level distributions, and then we integrate over the pdf of system load events in year i:

$$R_p^{PV}(i) = \int_{\overrightarrow{S}(i)} \sum_{k=1}^{K} f'_{\overrightarrow{S}(i)}(h_k) \cdot p_{f|h_k}(i) \cdot d(h_k(i)) \cdot \exp(-I_d \cdot r' \cdot i)\, d\overrightarrow{S}(i) \tag{8}$$

In which:

$R_p^{PV}(i)$	The present value of flood risk for the entire portfolio of dikes in the system in year i	€, *victims*
$f'_{\overrightarrow{S}(i)}(h_k)$	The probability density function of system loads in year i, causing local water levels (h_k) at dike section k taking into account the effect of breaches elsewhere in the system	–

3.3. Interventions in system

Different asset managers may differently apply intervention criteria and conditions, leading to different plans. Common steps are inventory of possible interventions, prioritisation, and planning them in time. In this paper, the first step is narrowed to dike reinforcement. The intensity of the intervention depends on the performance level which is pursued [31]. For the second step, the determination of prioritisation, the effect of the possible interventions is ranked. Several metrics may be used to rank the different options. In this study, we used three of them. The first metric reflects the distance of the actual safety of the dike section to a safety standard:

$$\forall k: \ ratio\ P(k,i) = \frac{P_{f_k}(i)}{P_{f_k\ standard}} \tag{9}$$

In which:

$P_{f_k\ standard}$	The standard for the acceptable probability of flooding of a dike section k	per year

A second metric enables to ranking of the risk effects of an intervention on system performance. For each dike section k the risk contribution from Eq. (6) is re-calculated with a simulated reinforcement in year i with a design horizon $i + T_{plan}$. For all dike sections, the differences are calculated between the risk in the actual state and the risk in the potential reinforced state of dike section k. It reflects the risk difference due to breaching of a dike section before and after a measure to meet the standard:

$$\forall k: \ \Delta R^{PV}(k,i) = R^{PV}(k,i) - R^{PV}\left(k_{reinforced}, i\right) \tag{10}$$

In which:

$\Delta R^{PV}(k,i)$	The difference between the present value of the flood risks of the potential reinforced and the actual dike section k in year i	€, *victims*
$R^{PV}(k_{reinforced}, i)$	the present value of the potential reinforced dike section k in year i, reinforced to be compliant until a year $i + T_{plan}$	€, *victims*

A third metric is the ratio between benefits and costs, in which the benefits of a measure are the corresponding decrease of the present value of the risk in Eq. (6):

$$\forall k: \ BC(k,i) = \frac{\Delta R^{PV}(k,i)}{C_k(i)} \tag{11}$$

In which:

$BC(k, i$	The ratio between the benefits of reinforcement of dike section k and the corresponding costs in year i	€
$C_k(i)$	the present value of the potential costs of dike section k in year i, reinforced to be compliant until a year $i + T_{plan}$	€, *victims*

The third step, planning the actual measures in the system in time based on the ranking derived in the second step, contains a check whether a planning criterion is met (e.g. exceedance of safety level), and a check on planning constraints such as available budget per year to perform an intervention. Starting with the measure with the highest rank, the measures with lower ranks can be taken as long as the planning criterion and constraints are met. The reinforcements $\Delta h_k(i)$ are solved with Eqs. (2)–(4).

Therewith the discounted risks in a year in Eq. (8) can be calculated and summed over years i until t_L like in Eq. (1):

$$R_p^{PV} = \sum_{i=1}^{t_L} R_p^{PV}(i) \tag{12}$$

In which:

R_p^{PV}	The present value of flood risk for the entire system over the period of interest, taking into account the system effects of the entire portfolio of dikes in the system	€, *victims*

4. Case study model

The model in Section 3 is built and applied on a case study: the Rhine River area in the Netherlands, see the red box in Fig. 5. For centuries, the Dutch policy has been to secure the country by dikes. The strategy is to standardize the dike safety level, based on risks, and to pursue compliance to that level. The standards have been set recently [36], based on risks per dike segment [29]. Furthermore, the strategy is to maintain safety levels by dike reinforcement taking into account ageing and climate change. About 1500 km of the dikes is not compliant with these standards [25]: the system is not in balance. The dutch Flood Protection Programme has been installed to reinforce dikes (in Dutch called 'HoogWaterBeschermingsProgramma', abbreviated as HWBP). The reinforcements in the Rhine River area are a major part of HWBP.

4.1. Physical system

The case study area in the red box in Fig. 5 is schematised in Fig. 6. The named blue lines are the river branches. The polders along the branches are presented as green boxes. Each polder can be flooded via one of the potential dike breach locations.

The main loads are represented by water levels. The strengths of the dike sections are represented by fragility curves. The water levels in

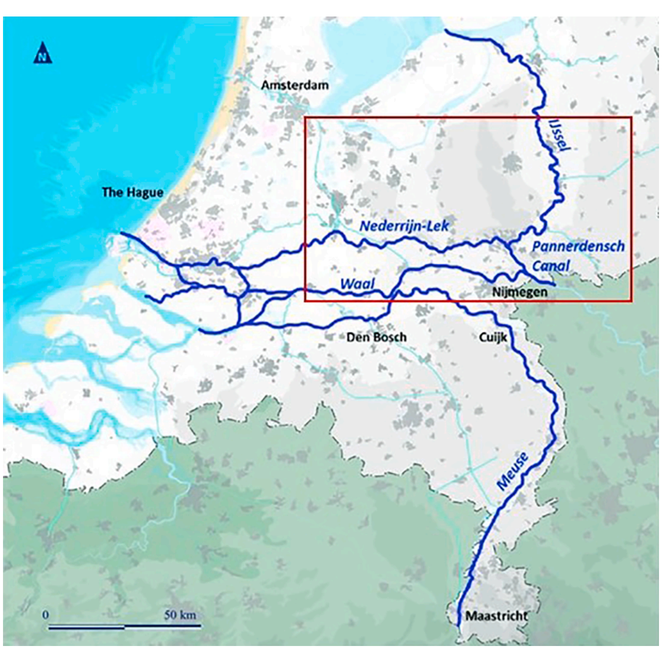

Fig. 5. Overview of the study area of the Rhine and its branches (in red).

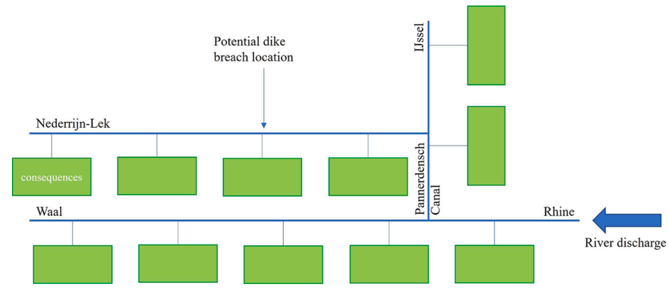

Fig. 6. Overview schematisation of the Rhine, its branches, potential breach locations, and the polders in which consequences occur in case of floods.

river branches depend mainly on the discharge of the main branch. The translation from these system loads $\vec{S}$ to local water levels is modelled by analytical relationships, which are based on available numerical simulations [1]. The local water level corresponding with the flood wave maxima is added with a model uncertainty factor.

$$\hat{h}_k = g_k(\hat{Q}_u(m_Q)) + m_h \tag{13}$$

In which:

$\hat{Q}_u$	Upstream discharge	m^3/s
$g_k(\hat{Q}_u)$	Local water level maximum at dike section k for a discharge $\hat{Q}_u$ based on [1]. These levels are given relative to the Dutch reference level NAP (in Dutch: Normaal Amsterdams Peil)	$m+$ NAP
$\hat{h}_k$	Local water level maximum at dike section k during flood wave	$m+$ NAP
m_h	Unbiased model uncertainty of local water level	m
m_Q	Unbiased statistical uncertainty of upstream discharge	m

The consequences of failure of a dike section are based on the results of about 1800 flood calculations [23], performed until the year 2015. In the Rhine River area upstream from influence by sea water levels, calculations are available for 63 potential breach locations in 24 dike segments, see Fig. 7. A dike segment is a length of dikes of about 25 km which is standardized in the Dutch law. A dike segment consists of different dike sections. In this study, the separation between dike sections is chosen between these breach locations because for further detail no flood calculations would be available. For each location are one or more records of consequences available (damage and victims) resulting from a breach occurring at a water level referred to with a return period. We assessed these return periods with the pdf based on the year 2015. Due to the effects of climate change, the return period of these water levels will decrease for events in years after 2015.

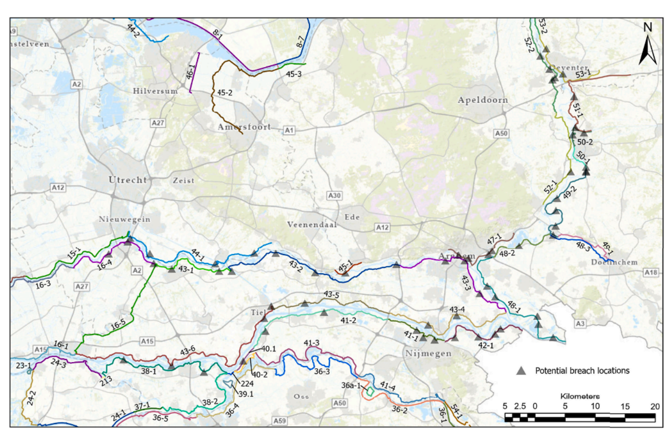

Fig. 7. Segments (coloured and numbered lines) and breach locations (grey triangles) in the study area.

Furthermore, the local water level is influenced by upstream disturbances due to breaches. In that case, a part of the discharge flows into an upstream polder, causing a decrease of the maximal water level downstream. The derivation of the correction for these situations is based on the law of preservation of discharge in the river branch where the breach takes place:

$$\widehat{Q}_u \cdot b_Q = Q_{b,\,downs} + Q_{breach} \tag{14}$$

In which:

Q_{breach}	Breach discharge into the polder, see Eq. (7).	m^3/s
b_Q	Fraction of discharge Q_u flowing into branch b.	–
$Q_{b,downs}$	Discharge downstream of a breach in branch b.	m^3/s

The downstream water level h_k at breach location k is determined with the analytical relations in [1] for which numerous numerical SOBEK calculations have been carried out, based on the upstream Rhine discharge. In Eq. (14) the local water level h_k is the only unknown in both $Q_{b,downs}$ and Q_{breach}, which can be iteratively determined. Note, a breach in one of the branches is assumed to not affect the discharge in the other branches, which assumption neglects the more complex effects near bifurcation points.

A typical result for the water level along a river branch is presented in Fig. 8. The blue line is the undisturbed water level, representing the situation without dike breaches. The dots on this line represent the potential dike breach locations on both sides of the river branch. The orange dots represent a Monte Carlo draw from the fragility curves, which characterise dike strength for that specific draw. The draws at each potential dike breach location along the river branch are independent and its course therefore looks random. The flood wave, propagating from upstream, first exceeds at km 887.5 an orange dot (strength). There a dike breach occurs, affecting the downstream water levels, represented by the grey line. Further downstream, between kilometers 910 and 920, two orange dots are below the undisturbed water level again, but no second breach occurs, because these dots are above the disturbed water level. Would one of them have been drawn below the disturbed water level, a second breach would have occurred. In that case, the process to find the downstream discharge and the water level at the breach with Eqs. (7) and (14) is carried out again. In this way, each drawn event is processed from upstream to downstream to find the accompanying breaches and water levels in the system.

4.2. Probabilistic model

4.2.1. Risks per year

The stochastic load variables are the yearly maximum river discharge ($\widehat{Q}_u$), the statistical uncertainty of its distribution (m_Q) and the model uncertainty (m_h). The stochastic strength variables are the fragility curves for the 63 potential breach locations.

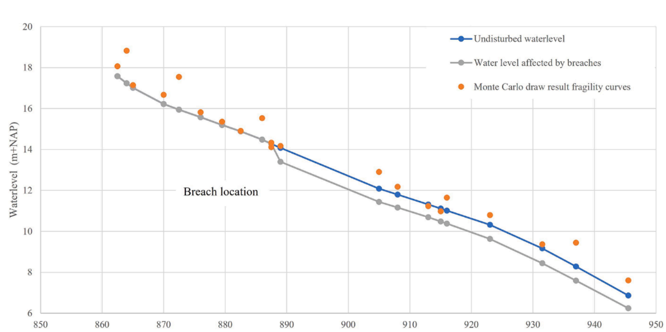

Fig. 8. Typical course of water level along the branch Rhine-Waal (see Figs. 5 and 6.

For the system risk assessment, a Monte Carlo Important Sampling method (MC-IS) has been used. This is an accurate method because flooding in a river area is only possible at large discharge. In Fig. 9 the flowchart of the calculations is presented. The central column is the core of the flowchart, containing a yearly update of the location of the fragility curves corresponding to Eq. (3), risk calculations and a propagating prioritisation and planning.

For a system consisting of one dike section and one breach location, the portfolio analysis for year i is a calculation of Eq. (8) with K=1. Firstly, we perform a draw from the pdf of the stochastic load variables, translate them to a local load $h(i)$ with Eq. (13), and draw from the fragility curve for the dike section representing dike strength ($h_{frag}(i)$). Secondly, the risks in year i are weighed and summed over all N events. Therewith, the calculation scheme for Eq. (8) is

$$R_p^{PV}(i) = \frac{\sum_{n=1}^{n=N} I_{MC}(n,i)\cdot w(n)\cdot d(h(n,i))}{\sum_{n=1}^{n=N} w(n)}\cdot \exp(-I_d\cdot r'\cdot i) \tag{15}$$

In which:

$I_{MC}(n,i)$	Indicator function indicating whether draw n leads to failure in year i: I=0 if $h(n,i) < h_{frag}(n,i)$ and I=1 if $h(n,i) > h_{frag}(n,i)$.	–
$h(n,i)$	Local load for the dike section in a system based on draw n from ($\widehat{Q}_u$, m_Q, m_h), in year i	$m+$ NAP
$h_{frag}(n,i)$	Draw n from the fragility curve for the dike section in the system, in year i	$m+$ NAP
$w(n)$	Weight of the n^{th} MC-IS draw event of the river discharge $\widehat{Q}_u(n)$: the probability density of that river discharge event divided by the probability density of the sampling function for that event.	–
N	Number of draws	–

For a system consisting of multiple interdependent dike sections, the first step is the same, except the draw is performed from the fragility curves for all dike sections in the system. A second step is inserted: a system analysis is performed to determine where the breaches would occur for this drawn event, and to adapt the downstream local water levels, see Fig. 8. Third, the risks per dike section k in year i are calculated based on the adapted water levels, summed over the system, weighed and summed over all N events. The calculation scheme for Eq. (8) is

$$R_p^{PV}(i) = \frac{\sum_{n=1}^{n=N}\sum_{k=1}^{K} I_{MC}(n,k,i)\cdot w(n)\cdot d\left(h_k'(n,i)\right)}{\sum_{n=1}^{n=N} w(n)}\cdot \exp(-I_d\cdot r'\cdot i) \tag{16}$$

In which:

$I_{MC}(n,k,i)$	Indicator function indicating whether draw n leads to failure in dike section k in year i: I=0 if $h_k'(n,i) <$ $h_{frag_k}(n,i)$ and I=1 if $h_k'(n,i) > h_{frag_k}(n,i)$.	–
$h_k'(n,i)$	local load for dike section k based on draw n from ($\widehat{Q}_u$, m_Q, m_h), in year i, adapted for breaches upstream	$m+$ NAP
$h_{frag_k}(n,i)$	draw from the fragility curve for dike section k in the system, in year i	$m+$ NAP

4.2.2. Failure probabilities on different scales

In this paper, we used dike sections defined in between the potential breach locations, with average lengths of about 8 km. For different reasons, we enabled the translation of probabilities of failure for different dike lengths:

- We used the actual failure probabilities as input for the derivation of realistic fragility curves, which are available per dike subsection in Vergouwe [61] with lengths of about 1 km
- The reinforcements are based on the standards, expressed as probability of failure, which are defined per dike segment, with lengths of about 25 km.
- The check of the risk-calculations is based on the system analyses in Vergouwe [61], which are based on detailed probabilistic modelling

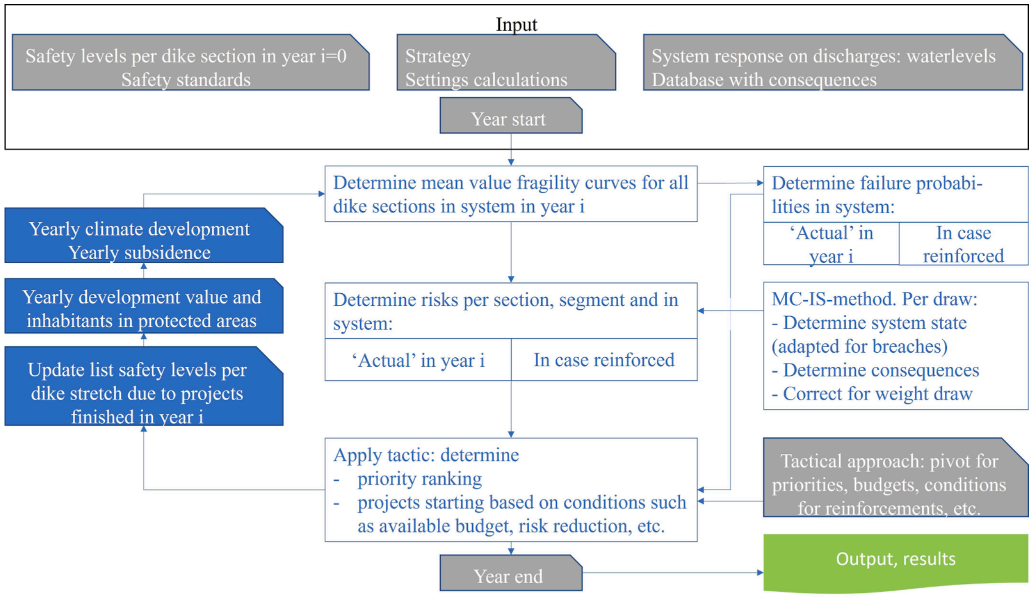

Fig. 9. Flowchart of the calculations for portfolio management of dikes. Input in grey, updates in blue, calculation steps in white, and results in green.

[53]. These are provided for entire polders, with dike lengths up to 200 km.

For this translation, we used an approximation which is rather good for small and not fully dependant probabilities of failure [60]:

- full dependence for the translation between dike subsections and dike sections, for which the correlation is very large,

$$P_{f_k}(i) = \max_{1 \le s \le m} P_{f_s}(i) \tag{17}$$

In which:

$P_{f_s}(i)$	The probability of failure of a dike subsection s in year i	–

- independence for the translation between dike sections and dike segments:

$$P_{f_j}(i) = 1 - \prod_{\forall k \in j} \left(1 - P_{f_k}(i)\right) \tag{18}$$

In which:

$P_{f_j}(i)$	The probability of failure of dike segment j in year i	–

To compare the results of these approximations with the system analysis in Vergouwe [61], we translated the results per dike segment to an entire polder similarly:

$$P_{f_{polder}}(i) = 1 - \prod_{\forall j \in polder} \left(1 - P_{f_j}(i)\right) \tag{19}$$

In which:

$P_{f_{polder}}(i)$	The probability of failure of a polder in year i	–

We applied these translations to those polders in the study area for which Vergouwe [61] determined failure probabilities. The comparison is rather good, see Fig. 10.

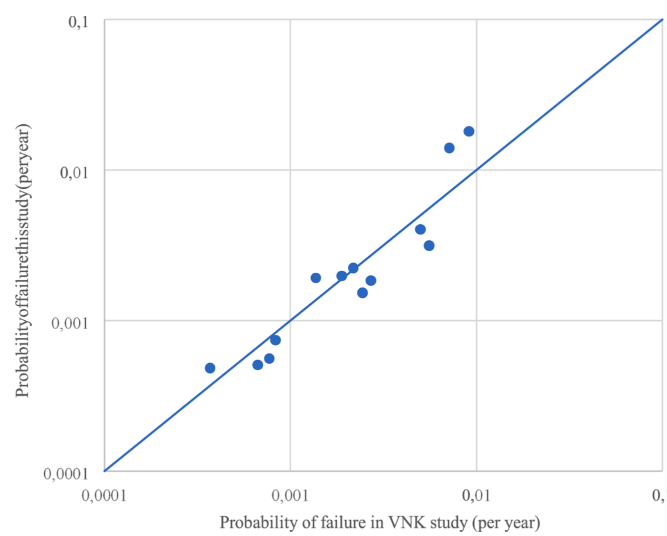

Fig. 10. Comparison between the results in Vergouwe [61] (denoted as VNK study) for 13 polders (38, 40, 41, 42, 44, 45 and 47–53) and the approach in this study.

4.3. Derivation of probability density functions over time

The pdf's for loads and strength in Eq. (8) are time dependant. The system loads $\overrightarrow{S}$ are represented by river discharge. The strengths by fragility curves.

4.3.1. River discharge

In a riverine area, the maximal river discharge during a flood wave is the most important stochastic variable to assess flood risks. The representation of the pdf of the discharge of the Rhine River at the border of the Netherlands is given in [9]. In this paper, this river discharge $\widehat{Q}_u$ is represented by a Gumbel distribution, transformed as described in detail in den Heijer and Kok [13] (par 9.2 of the supplementary material) to get a realistic pdf in the time frame of the case study.

4.3.2. Fragility curves

The fragility curves are required for the actual situation (I=0) and for reinforcements in year i to solve Eqs. (3) and (4). However, not in all cases fragility curves are available since flood probabilities can be derived via other methods than Eq. (2), such as [61] which provides probabilities of failure per dike section. For testing the proof of concept in this paper we used these probabilities as a starting point for the derivation of the fragility curves. We used a normal distribution like Fig. 4. Given this shape, the required fragility curves are represented by $\mu_{frag_k}(0)$ and $\mu_{frag_k}(i+T_{plan})$ for the actual and reinforced situation respectively.

For the actual situation (I=0) we merged the available results per dike subsection in [61] to the larger dike sections we used based on full dependence within the dike section, see Eq. (17). For the derivation of the fragility curve for reinforcements in year $i + T_{plan}$ the probability of failure per dike section is obtained from the standards for flood probabilities which are to be met per dike segment $_j$, consisting of several dike sections. The flood probabilities per dike section k are obtained based on independence between the dike sections in the dike segment, see Eq. (18), which for small probabilities is approximated by:

$$P_{f_k}(i) = P_{f_j}(i)\cdot\frac{L_k}{L_j} \tag{20}$$

In which:

L_j	length of dike segment j	km
L_k	length of dike section k	km

For both the actual and the reinforced situation a Newton-Raphson method is used to solve the location $\mu_{frag_k}(i)$ iteratively, leading to these probabilities of failures for dike section k in Eq. (2). As a heuristic prior estimate herein the water level is used which corresponds to an exceedance frequency equal to the actual probability of failure. In each iteration numerical integration is used to solve Eq. (2).

4.4. Budget and costs over time

The budget for measures is calculated as the base budget at the start of the period of interest, increased with inflation:

$$B(i) = B(i=0)\cdot(1 + infl)^i \tag{21}$$

In which:

$B(i)$	The budget for flood risk measures in year i	€
$B(i = 0)$	The yearly budget for flood risk measures at the start year of the analysis $i = 0$	€
$infl$	yearly inflation	–

The costs of measures are based on key numbers for saving tenfold [50], again corrected for inflation:

$$C_k\left(i, T_{plan}\right) = f_C(k,i)\cdot\left(\frac{\Delta h_k(i)}{h_k^{10}}\right)\cdot C_k^{10}\cdot L_k\cdot(1 + infl)^i \tag{22}$$

In which:

$C_k(i, T_{plan})$	The cost of a reinforcement in year i, targetting to reinforce for the year $i + T_{plan}$	€
h_k^{10}	Water level difference with a tenfold decreased probability of exceedance	m
C_k^{10}	Costs per km for dike reinforcement required for a tenfold decrease in probability of flooding	€/km
$f_C(k,i)$	Reduction factor on costs for dike section k in year i	–

The actual strengths may vary significantly along a dike section [61]. Therefore, since some parts should be more reinforced than others, the costs $C_k(i, T_{plan})$ are reduced by f_C when the dike section is reinforced for the first time in the simulation period. The reduction is approximated based on the proportionality of reinforcements $\Delta h_k(i)$ to $\log P_{f_k}$, which is in line with the use of an extreme value distribution for discharges and water levels:

$$f_C(k,i) = 1 - \frac{\sum_s \frac{L_s}{L_k}\cdot\left(logP_{f_s} - log\max_s P_{f_s}\right)}{logP_{f_{k,standard}} - log\,P_{f_k}(i)} \tag{23}$$

In which:

L_s	Length of dike subsection s	m
$P_{f_{k,standard}}$	The standard for dike section k based on the formal standard for dike segments by Eq. (20)	–

Fig. 11 provides a schematic representation of the cost reduction. The counter in Eq. (23) sums a length-weighed distance to the maximal probability of failure, the lowest point in Fig. 11, represented by arrow (2). The denominator represents the distance between the actual and required probability of failure, which is arrow (1). Note, due to unknown years of the different interventions, in advance it is unknown at what actual safety level $P_{f_k}(i)$ the intervention will take place. Therefore, the denominator of the reduction factor f_C is dependant on the year $_i$.

5. Application and results

5.1. Numerical settings and model check

Several model runs have been carried out to choose numerical parameters leading to stable flood risk calculations. The performance of the case study model is compared with the results of a detailed national study (from here denoted as VNK) on actual risk assessments in the Netherlands [28,61]. VNK provides probabilities per polder, which are in most cases enclosed by several dike segments. Each polder consists of dozens of small dike sections delivering a high level of detail for assessment of actual safety. For the comparison in this section, the starting points of the calculations in VNK [61] are used. For the year of comparison 2015 is chosen, the year VNK reported. We used the results for 5 polders which are entirely in the model area (see Fig. 6). Table 1 provides the starting points for the comparison, the pdf's for probabilistic calculations, and the numerical parameters.

The results are shown in Fig. 12. The comparison is good for flood probabilities (grey), economic risks (blue) and risk on victims (yellow).. Thus, despite the use of a less detailed dike section schematisation, a hybrid numerical analytical modelling of the water levels in the river system, probabilistic modelling without dependency between dike sections, and a calculation of consequences for each MC draw instead of only a few, the results are comparable. This comparison serves as a check for the modelling and implementation.

Since the standard deviation of the fragility curves ($\sigma = 0.50_m$) is based on expert opinion, we examined the effects of different values of the standard deviation used in the fragility curves. The comparison for $\sigma = 0.25_m$ is more or less the same and for $\sigma = 1.00_m$ it is significantly less. Therefore, we kept $\sigma = 0.50$ m.

5.2. Elaborative calculations

Some elaborative calculations are made to get an understanding of

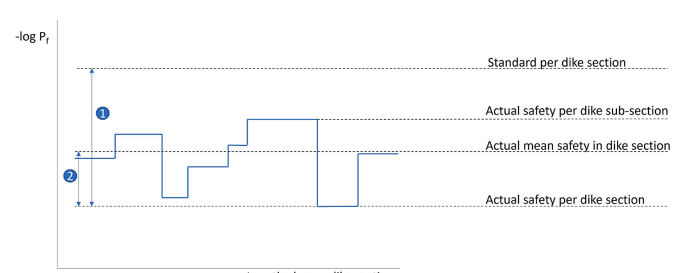

Fig. 11. Schematic cost reduction due to existing differences in safety level along dike sections.

Table 1
Overview of numerical starting points for the case study model, and the adapted case study specific ones for a proper model check with VNK.

Starting points	Case study (Sections 5.2 and 5.3)	Model check (only Section 5.1)
System effects on probabilities of failure due to breaches upstream polder	Yes	No
Evacuation fraction	56% [50]	
Database with consequences [23]	For water levels higher than the highest in the database, the consequences corresponding to the highest water level are chosen. For water levels lower than the lowest in the database, the consequences are truncated to zero	
Value of a human life (per victim)	6,7 M€ [29]	Neglected
Consequences (per affected person)	12,500 € [29]	Neglected
Sampling Function (SF) for $\hat{Q}_u$	Normal distribution with (μ,σ) is (16,000,2000) m^3/s	
Number of draws	10,000	
m_h	Normal distribution with (μ,σ) is (0,0.15) based on [15,51] truncated at $\mu - 2.9\sigma$ and $\mu + 2.9\sigma$	
m_Q	Normal distribution with (μ,σ) is (0,1) based on [9] and section 9.2 of supplementary material in [13], truncated at μ−2.9σ and μ + 2.9σ	
fragility curves	normal distribution with σ is 0.5m	
Step size $\hat{Q}_u$	$50m^3/s$	
Step size m_h, m_Q	$5/6 \cdot \sigma$	

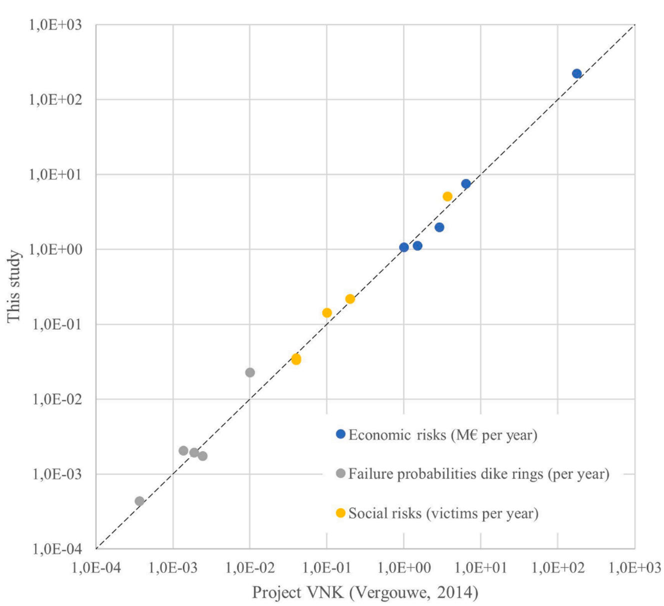

Fig. 12. Comparison model of this study with results of project VNK, dike ring areas 42, 43, 47, 48 (except dike segment 48–3), and 50 [61] for the probability of failure, economic risks and risks on victims. NB. the most right grey bullet would shift right a bit, because it is reported as '>0.01 per year' in Vergouwe [61].

the model behaviour and the results and tactical planning settings. In this subsection, the results for risks and costs are not discounted to get a clear insight into the course of the results in time. Table 2 provides the case-specific parameters which are used together with Table 1.

In Fig. 13 the model result is shown. The prioritisation of interventions is based on the maximum decrease in economic risks (see Section 3.3). Consequently, the economic risks (grey) decrease at each reinforcement. The cost increases at each reinforcement (brown) until all dikes reach their standard. The total budget (blue) is proportional and increases due to the yearly added budget and inflation.

In Fig. 14 the model result is shown for the situation as in Fig. 13, accepting overplanning as long as the execution costs (the last 2 years of each reinforcement, see Table 2) fit in the budget (grey). The risks are smoother in time, and even a small increase occurs around 2035, due to the fact a top-ranked dike cannot be reinforced due to budget shortage and a reinforcement upstream causes increased risks downstream. A variant in which the top 3 ranked dikes are forced to be planned first shows a more continuously descending course of risks in time (yellow), in this paper referred to as a priority condition. Before 2035 the risks of this variant are somewhat higher with respect to the grey line due to the fact no expenditures on other dikes are made before the top-ranked dikes are reinforced. After 2035 the risks are considerably lower.

In Fig. 15 the model result is shown in case of system changes in population growth rate, subsidence rate, and climate scenario (see Table 2 in time (grey). As a reference, the yellow line is the same as in Fig. 14. The risks show a clear difference. Just from the start in 2015 they increased, because the first reinforcements only become effective after the construction period of 7 years. From 2022 they decrease, however, considerably higher risks are present, and more time is needed to reduce the risks until they stabilize around 2080. The costs consequently follow the budget during this time. The stable risk level of the variant with changes (grey, after 2080) is some lower than that of the completely stable variant without system changes (yellow), for which the reinforcements will lead to an exactly compliant system. This is because, in a changing system, a reinforcement meant to be compliant with circumstances a design horizon ahead leads to a surplus of risk reduction at the time of reinforcement. Over the full portfolio, this leads to some extra risk reduction.

Table 2
Overview of case study specific starting points.

Starting points	Case study (Sections 5.2 and 5.3)
Period of analysis	100 years, starting from 2015
Breach width and depth	150 m based on historic floods [62], head $h_k - h_{bk}$ of 5 m based on the extreme water levels and polder levels in the study area
Population growth rate	0,33% per year
Subsidence rate	0.1 m per 50 years
Climate scenario	G+ [59]
Budget at the start of the analysis	The budget is based on the national budget of HWBP of 362 M€ per year. Since the study area contain 498.9 km from the national 3437 km of dikes, the length-proportional budget is taken as 50 M€ per year, in this paper referred to as the proportional budget.
Reinforcement cost division over preparation and execution years	HWBP pursuits reinforcement in 7 years. Five preparation years are used together for 25% of the cost. In the last 2 execution years the actual reinforcement takes place, using the other 75%.
Costs per reinforcement unit C_k[10] (in equation (22))	[50]
Cost reduction factor f_C	correct costs of first reinforcement for dike sections in which actual safety level differs along the length, minimized by a chosen value of 0.25 for minimal required fixed costs
The price level at the start	2015
Inflation	2%
Discount	5% (2% in section 5.2)

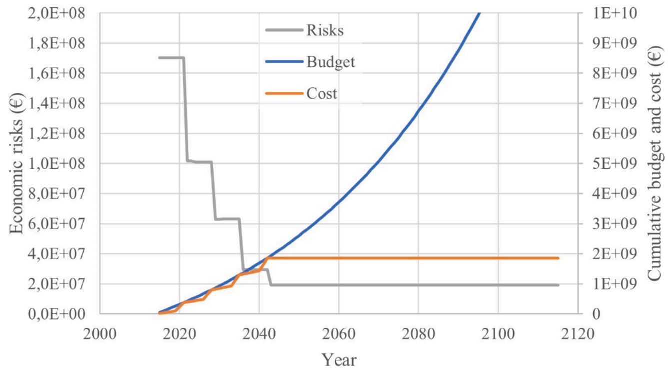

Fig. 13. Model result for general starting points, for prioritisation based on decrease of economic risks.

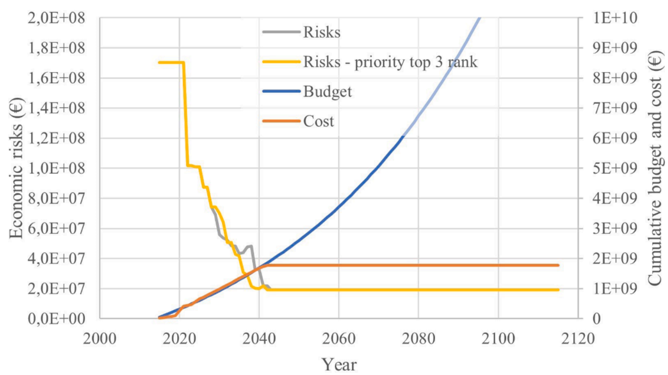

Fig. 14. Model results as in Fig. 13 and planning with tolerance for overplanning (corresponding risks in grey) and a priority condition for the top 3 ranked dikes (corresponding risks in yellow).

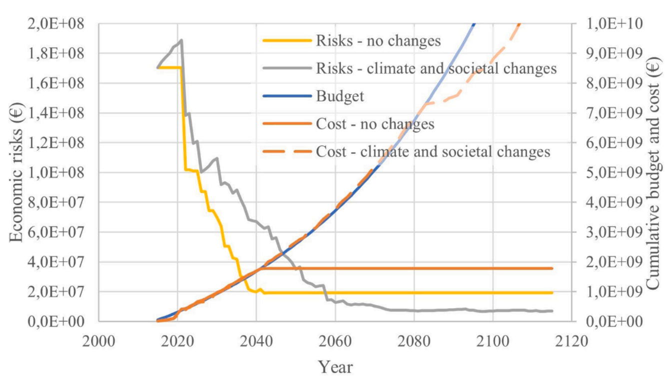

Fig. 15. Comparison of model results without (yellow, as in Fig. 15) and with system changes (grey).

In Fig. 16 again the model result is as in Fig. 15 (grey). The effect of a physical discharge limit of 18,000 m^3/s due to breaches upstream of the study area is presented as well (yellow). Although the effect is not that large, we use this discharge limit, since it is more realistic and in correspondence to this research on system effects.

In Fig. 17 the model results are presented for different prioritisation metrics in Section 3.3: decrease of economic risk (yellow), societal risk (black, right axis), safety performance (green) and benefit cost ratio (grey). The course of the risks in time is comparable.

All incremental changes in the presented results of the elaborative calculations develop in time in an understandable course. This serves as a second check on the proper implementation, next to the comparisons with [61] in the previous subsection.

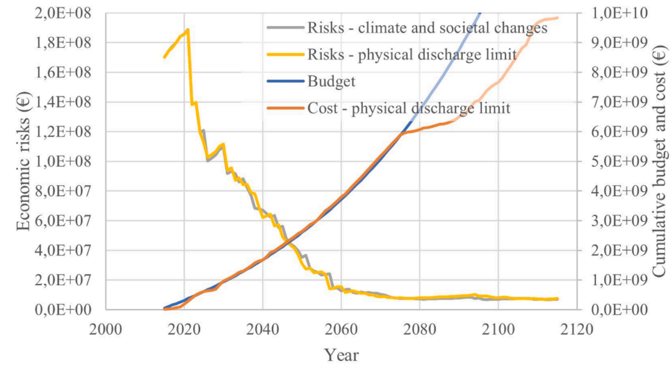

Fig. 16. Model results without (grey, as in Fig. 15) and with a physical river discharge limit (yellow).

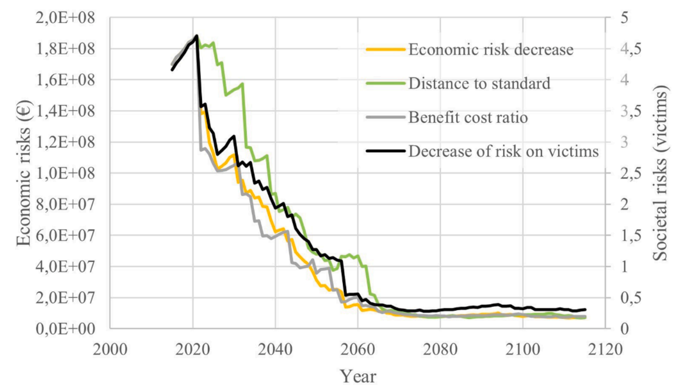

Fig. 17. Model result for different prioritisation metrics: Economic risk decrease (as in Fig. 16, yellow), Distance to standard (green), Benefit cost ratio (grey) and Decrease of risk on victims. The first three refer to the left axis, the last to the right axis.

5.3. *Results for different tactical management plans*

A tactical management plan defines the planning of consecutive measures to implement a strategy. Tactical plans may differ due to several choices such as:

- The criterion to include reinforcement in the program planning, e.g. exceedance of a safety level.
- Metric for prioritisation: order on decreasing risk reduction per year, on decreasing differences between actual and required safety level, or on benefit-cost ratio.
- A priority condition is to give priority to plan a number of top-ranked dikes first, which holds no others are planned as long as for these dikes is no room on programme.
- Available budget per year, and the division of the budget over the period of interest
- Minimal risk reduction rate per reinforcement is relative to the measure with maximum risk reduction in a year, to postponing the reinforcements which have small risk effects.
- Planning window shifting through the period of interest (see Fig. 2). In planning, this is the time for which reinforcements were actually planned and executed.
- The degree of reinforcement. In some models, the intensity of reinforcement is a degree of freedom [69], or partial reinforcement is enabled [31].
- Design horizon of a reinforcement.
- Provisions for overplanning: In most models the budget limits all activities, however, in practice mostly at least preparations for the next projects are allowed because of low costs.

- Intangible starting points such as to pursue regional spread.

HWBP is actually active in the case study area and uses a mix of different tactics for planning: difference between actual safety and standard, regional spread, and available budget per year. In this study, we defined different tactical plans based on the list above. The first item in the list is fixed, because the criterion for planning is based on the Dutch strategy, which holds that a dike can only be planned on the programme when the safety standards are exceeded, indicating dike reinforcement is needed shortly. The second, third and fourth item is varied as provided in Table 3 because these appeared to be important in elaborative calculations. For the other items a single starting point is taken, see Table 4.

These variations together lead to $3 \times 2 \times 2 = 12$ different tactical plans. Two other variants are calculated which are in fact no realistic tactical plans: the 'do nothing' option representing the growing risk over time, and the option with infinite budget leading to reinforcement of all dikes at once after the 7-year preparation period. All tactical plans are presented in Table 5. In Table 6 the results of all tactical plans are provided.

Fig. 18 summarizes the results for all tactical plans except 13 and 14. The horizontal axis represents the expected number of victims in the simulation period of 100 years. The vertical axis contains the discounted value of the sum of costs and economic risks in the same period.

The difference between the total present value of costs and risks for the 'do nothing' option (tactical plan 13) and plans 1–12 reflect the effect of the flood risk strategy to ensafe the area, on an average about 50%. The social risk is reduced by on an average about 85%. The differences between the tactical plans 1–12 are up to 40% for the total present value and up to 70% for social risk, which is the same order of magnitude as the effect of the flood risk strategy. Especially the differences caused by the prioritisation metric and priority condition are significant. Fig. 19 shows that a risk based prioritisation metric in combination with a priority condition for the top 3 ranked dikes (the two most right orange bars) has about the same effect on cost and risk as doubling the budget in combination with a safety-level based metric (left yellow and grey bar).

6. Discussion

In this section, we discuss consecutively critical assumptions, extensibility, application and practical implications with respect to the presented methodology and application.

6.1. Assumptions

The type of flood risk intervention we considered in this paper is dike reinforcement. During the simulation, we yearly assessed the probability of failure with fragility curves. A prerequisite for the application of the methodology is the availability of existing actual fragility curves or actual failure probabilities per dike subsection. In countries where these quantities are used to meet design standards, such as the UK, Germany and the Netherlands, these are available, because prior to the planning process, these are part of the dike condition examination. The same prerequisite holds for a hydraulic model to translate system loads to local loads, and consequence calculations for representative breach locations. In the case study, we tuned the actual fragility curves in a way the probabilities per dike section at the start of the analysis are aligned with VNK [61].

The fragility curves for to-be-reinforced dikes can be determined in several ways. In this paper we used the shape of the fragility curves in the actual situation and shifted them based on climate change and subsidence to get a provisional fragility curve for a future situation, solving the Eqs. (4), (3) and (2). An alternative approach would be to pro-forma-design conform design standards and derive a fragility curve, which would need detailed information and calculations. Another

Table 3
Overview of varied aspects of the tactical plans implemented in the model.

Metric for prioritisation	Budget	Priority condition
Based on safety performance, see Eq. (9)	Proportional budget for case study area wrt to the national budget, in 2015 50 M€	No further planning restriction
Societal risk-based, see Eq. (10) (also applicable for economic risk effect)	Double budget for case study area: In 2015 100 M€	Top 3 rank first, postponing other measures
Based on benefit cost ratio, see Eq. (11)		

Table 4
Overview of starting points for parameters in the tactical plans implemented in the model.

Parameter	Used in this study
Planning criterion	The probability of failure of the dike segment exceeding the standards, and the probability of failure of the dike section exceeding its length-proportional value calculated with Eq. (20).
Minimal risk reduction rate	0 (which means: no)
Planning window	12 years
Reinforcement	Standard level at design horizon
Design horizon	50 years
Overplanning	Allowed for the preparation years of a reinforcement
Intangible aspects	No

Table 5
Overview of tactical plans implemented in the model, composed of the different decision rules in Table 3.

Tactical plan	Metric for prioritisation	Budget	Priority condition
1	safety level	Proportional	no
2	safety level	Proportional	top 3
3	safety level	Doubled	no
4	safety level	Doubled	top 3
5	societal risk level	Proportional	no
6	societal risk level	Proportional	top 3
7	societal risk level	Doubled	no
8	societal risk level	Doubled	top 3
9	benefit-cost ratio	Proportional	no
10	benefit-cost ratio	Proportional	top 3
11	benefit-cost ratio	Doubled	no
12	benefit-cost ratio	Doubled	top 3
13	economic risk level	0	top 3
14	economic risk level	∞	top 3

Table 6
Overview of results for all tactical plans in Table 5.

Tactical plan	Present value risk (billion €)	Present value cost (billion €)	Total present value (cost and risk, (billion €)	Societal risk (no. of victims)
1	4.27	1.47	5.74	226
2	3.38	1.47	4.85	159
3	2.12	1.86	3.98	86
4	1.95	1.88	3.83	81
5	3.18	1.47	4.64	180
6	2.73	1.46	4.18	126
7	1.84	1.87	3.71	78
8	1.80	1.88	3.68	76
9	3.44	1.47	4.91	184
10	2.59	1.48	4.07	125
11	1.80	1.87	3.67	79
12	1.78	1.88	3.66	77
13	8.15	0.00	8.15	972
14	1.36	2.05	3.42	59

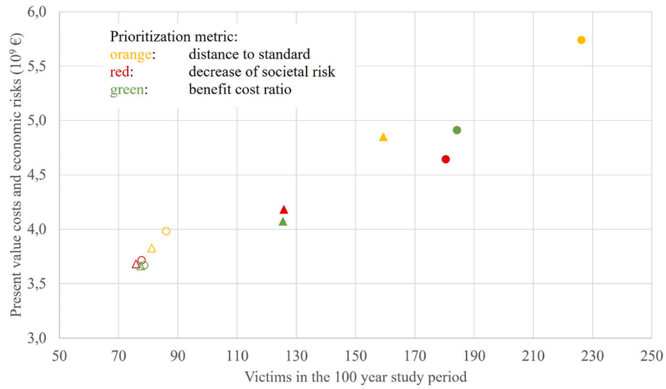

Fig. 18. Model result for tactical plans 1–12, with the budget denoted by filled (proportional budget) or open marker (doubled budget), the prioritisation metric denoted by colour, and the priority condition denoted by marker shape (dot: no; triangle: top 3 first).

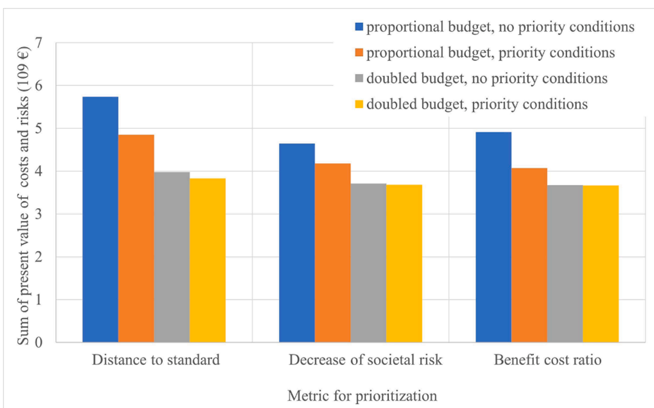

Fig. 19. Overview of present values of cost and risk for tactical plans 1–12.

alternative could be to use a class of standard fragility curves for different typologies of reinforcements, such as adapted dike slopes. These alternative approaches would need a similar approach as used in the present paper to enable to shift the re-shaped fragility curve until it meets the standard at the design horizon.

For estimations of the effects of breaches on downstream river loads, we neglected the backwater effect in the polders. This is sufficiently accurate in case of critical flow through the breach. This holds in the initial phase of the flooding, which phase is assumed to be most important for the reduction of the event water level maxima downstream. Additional calculations are executed to examine the sensitivity of the downstream water level effect of breach widths on the system risks. They underpinned the low sensitivity for breach widths in the range of most historic observations in the Netherlands, 75–200 m [62].

A limitation of this concept is the effect of timing and growth of breaches on downstream river loads. They are assumed to occur suddenly at the water level maxima of floods. This overestimated the water level reductions downstream the river. Nevertheless, if no system behaviour is taken into account, the downstream water levels are certainly over-estimated. We recommend research with hydraulic and breach development model simulations, to investigate this time effect on the downstream water level reductions.

6.2. *Application and practical implications*

In the case study the probabilities of flooding are based on [61]. Herein, the residual strength, which is defined here as the strength of a dike after the occurrence of an initial failure mechanism, is not taken into account for the geotechnical mechanisms macro stability and piping, which may be important in the river area. Therefore, the probabilities are considered as an upper limit. For development of a method to compare tactical plans, the probabilities are considered to be sufficient.

The different tactical plans lead to different intervention schemes. To illustrate the effect of different prioritisation metrics and the priority condition, Table 7 presents the similarities and differences of the interventions in the first 15 years of the analysis for the tactical plans 1, 6 and 10 in Table 6. For all plans the length-averaged $\triangle h_k$ is similar. The breakdown of the reinforcement surface to branches shows clearly that the attention of the societal risk-driven intervention tactic (plan 6) is almost completely on dikes along the Waal (see Fig. 5), protecting large and deep polders from flooding. The Waal is the largest river branch of the Rhine River, and may cause flood depths with high risks to victims. The other two tactical plans 1 and 10 show more spread of the interventions over the river branches with a focus on the Nederrijn-Lek. Another difference, shown in the number of sections column, is the focus of plan 6 on the reinforcement of a limited number of important sections and the spread of investments over many sections in the other plans.

6.3. *Extensibility*

The methodology to compare tactical plans is developed to be generically applicable. The fragility curves and the intervention's decision rules are crucial elements. In the case study, we used a normal distributed fragility curve per dike section. Eq. (2) is suitable for other shapes, e.g. for a fragility curve composed of different failure mechanisms. The intervention decisions may be based on different design rules. In the case study, we used compliance with safety standards at the end of the design horizon. The methodology is suitable for other intervention rules or intensities as elaborated in [31] or e.g. for a fixed reinforcement step of a factor 10 in safety. Furthermore, this methodology is suitable for a cascade of strategies, e.g. to elaborate adaptive pathways of strategies [22]. Sub-paths in a pathway can be implemented as different tactical plans being effective in certain periods, translated into additional or changed intervention rules like Table 3.

In this study, the river discharge is the main stochastic variable determining the local water levels. The MC approach in combination with the physical river discharge model and consequence simulations integrates causal knowledge about a system with probabilistic and risk analysis techniques [41]. This enabled us to take into account breach effects on system loads without additional hydraulic calculations. The application can be extended to e.g. an area near sea, where the local water level is determined by river discharge and sea water level. In the case water levels are determined by multiple stochastic system load variables, additional hydraulic calculations for several different combinations of those variables are required to determine the system effects of a breach event. Since breaches near the sea have a limited effect on water levels at neighbouring locations compared with breaches in riverine areas, the system effects are expected to be smaller.

7. Conclusions

This paper focuses on the development and application of a methodology for the comparison of tactical plans for interventions in an interdependent system of dikes. We conclude that the developed model-based tactical planning approach is applicable in a riverine area, that tactical planning is important for the reduction of flood risks over time, and that the methodology is extendable to other water systems.

The methodology is applied to the system of dikes along the Rhine River branches in the Netherlands, taking into account deterioration due to subsidence, climate change and population growth. The case study shows the applicability of the methodology to calculate the portfolio metrics performance, risk and cost, which are key for mature asset

Table 7
Overview of reinforcements for tactical plans 1, 6 and 10 (see Table 5) for the reinforcements up to and including 2030. NB. The reinforcement surface is the dike length multiplied by the dike height increase.

	Reinforcements			Reinforcement surface per branch (*1000 m^2)				
Tactical plan	Length (km)	Length-averaged $\triangle h_k$ (m)	Number of sections (-)	Rhine	Waal	Pannerdensch Canal	Nederrijn- Lek	IJssel
1	140.1	1.13	26	3	48	14	**75**	19
6	103.6	1.33	10	0	**102**	13	22	0
10	183.0	0.85	24	17	41	13	**71**	14

management decisions [6,39].

Tactical planning is important to effectively and efficiently reduce flood risks over time to the compliant level. This is based on the calculation of the costs and risks over time for 12 different tactical plans for different prioritisation and planning considerations and different budgets. The results show the present value of the sum of costs and risks of the plans differ by up to about 40% with respect to that of the plan with the highest present value. For social risks, the differences are up to 70%. An example is that interventions based on a benefit-cost-ratio prioritisation in combination with the condition to reinforce the top 3 ranked dikes first (plan 10), have the same effect on cost and risk as decisions based on a probability-based prioritisation in combination with doubling the budget (plan 3). Furthermore, different plans lead to different patterns and intensity of measures in the system.

The application can be extended to other than riverine areas, which would need additional hydraulic calculations. System effects near the sea are expected to be smaller than the effects along rivers.

This paper underpins that the application of the presented methodology provides understanding that supports planning discussion and the corresponding tactical decisions. This study contributes to the work on model-based planning of interventions in large portfolios of interdependent assets.

CRediT authorship contribution statement

Frank den Heijer: Writing – original draft, Visualization, Software, Methodology, Investigation, Formal analysis, Data curation, Conceptualization. **Matthijs Kok:** Writing – review & editing, Supervision.

Declaration of Competing Interest

The authors declare that they have no known competing financial interests or personal relationships that could have appeared to influence the work reported in this paper.

Data availability

Data will be made available on request.

References

[1] Agtersloot R, van der Veen R, van der Veen SR. Betrekkingslijnen rijntakken, versie 2018 (Tech. rep.). RURA-Arnhem; 2019.
[2] Apel H, Thieken AH, Merz B, Blöschl G. Flood risk assessment and associated uncertainty. Nat. Hazard. Earth Syst. Sci. 2004;4(2):295–308.
[3] Bachmann, D. (2012). Beitrag zur Entwicklung eines Entscheidungsunterstützungssystems zur Bewertung und Planung von Hochwasserschutzmaßnahmen (Doctoral dissertation, RWTH Aachen). Retrieved from publications.rwth-aachen.de/record/64633/files/4043.pdf.
[4] Bachmann D, Huber NP, Johann G, Schüttrumpf &H, Schüttrumpf H. Georisk: assessment and management of risk for engineered systems and geohazards fragility curves in operational dike reliability assessment. Assessment and Management of Risk for Engineered Systems and Geohazards, 2013;7(1):49–60. Retrieved from, www.tandfonline.com/loi/ngrk20.
[5] Bachmann D, Schüttrumpf H. Integrating the reliability of flood protection structures into catchment-based flood risk analysis. Hydrol Wasserbewirtsch 2014;58(3):168–77. Retrieved from ISSN1439-1783.
[6] Brown, R.E., & Humphrey, B.G. (2005). Asset management for transmission and distribution (Vol. 3) (No. 3).
[7] Buijs F, Hall J, Sayers P, Van Gelder P. Time-dependent reliability analysis of flood defences. Reliab Eng Syst Saf 2009;94(12):1942–53. https://doi.org/10.1016/j.ress.2009.06.012.
[8] Carpitella S, Mzougui I, Benítez J, Carpitella F, Certa A, Izquierdo J, et al. A risk evaluation framework for the best maintenance strategy: the case of a marine salt manufacture firm. Reliab Eng Syst Saf 2020. https://doi.org/10.1016/j.ress.2020.107265.
[9] Chbab, E.H. (2017). Basisstochasten WBI-2017 - Statistiek en statistische onzekerheid (Tech. Rep.). 1209433-012-HYE-0007 Deltares.
[10] Courage W, Vrouwenvelder T, van Mierlo T, Schweckendiek T. System behaviour in flood risk calculations. Georisk: AssessManage Risk Eng Syst Geohazards 2013;7(2):62–76.
[11] Curran A. Flood risk analysis of embanked river systems - probabilistic systems approaches for the RHINE AND PO RIVERS. Doctoral dissertation. Delft University of Technology. Retrieved from ISBN978-94-6421-121-4.
[12] Deltacommissie. Rapport deltacommissie deel 1 - Eindverslag en interimadviezen (Tech. rep.). Den Haag: Staatsdrukkerij en uitgeverijbedrijf; 1960.
[13] den Heijer F, Kok M. Assessment of ductile dike behavior as a novel flood risk reduction measure. Risk Anal 2022:1–16.
[14] Domeneghetti A, Vorogushyn S, Castellarin A, Merz B, Brath A. Probabilistic flood hazard mapping: effects of uncertain boundary conditions. Hydrol Earth Syst Sci 2013;17(8):3127–40. Retrieved from, https://hess.copernicus.org/articles/17/3127/2013/.
[15] Duits, M. (2019). HYDRA-NL gebruikershandleiding, versie 2.7 (Tech. Rep.). PR4022.10, HKV lijn in water.
[16] Dupuits EJC, Klerk WJ, Schweckendiek T, De Bruijn KM. Impact of including interdependencies between multiple riverine flood defences on the economically optimal flood safety levels. Reliab Eng Syst Saf Retriev 2019. https://doi.org/10.1016/j.ress.2019.04.028.
[17] Eijgenraam C.J. Optimal safety standards for dike-ring areas (Tech. rep.). isbn 90-5833-267-5. CPB Netherlands Bureau for Economic Policy Analysis. Retrieved from www.cpb.nl. 2006.
[18] Eijgenraam CJ, Brekelmans R, Den Hertog D, Roos K. Optimal strategies for flood prevention. Manag Sci 2017;63(5):1644–56.
[19] Fluixá-Sanmartín J, Escuder-Bueno I, Morales-Torres A, Castillo-Rodríguez JT. Comprehensive decision-making approach for managing time dependent dam risks. Reliab Eng Syst Saf, 203; 2020. https://doi.org/10.1016/j.ress.2020.107100.
[20] Fuchs GH, Keuning I, Mante BR, Bakker JD. A business case of the estimated profit of life cycle management principles. In: Life-cycle of structural systems: design, assessment, maintenance and management – Proceedings of the 4th international symposium on life-cycle civil engineering; 2015.
[21] Guan X, Sun H, Hou R, Xu Y, Bao Y, Li H. A deep reinforcement learning method for structural dominant failure modes searching based on self-play strategy. Reliab Eng Syst Saf 2023;233:109093.
[22] Haasnoot M, Kwakkel JH, Walker WE, ter Maat J. Dynamic adaptive policy pathways: a method for crafting robust decisions for a deeply uncertain world. Glob Environ Chang 2013;23(2).
[23] Helpdesk Water. (2020). National database flood simulations. Retrieved 2020-08-27, from www.helpdeskwater.nl/onderwerpen/wetgeving-beleid/europese-richtlijn-overstromingsrisico/overstromingsgevaar-overstromingsrisicokaarten/.
[24] Hu Y, Peng Q, Ni Q, Wu X, Ye D. Event-based safety and reliability analysis integration in model-based space mission design. Reliab Eng Syst Saf 2023;229:108866.
[25] HWBP. (2022). HWBP-projecten, Samen Innoveren, 2023. Retrieved 2023-02-13, from https://drive.google.com/file/d/1PzV0-26u3lxvZIdzjJVmAbOhSGEX12MV/view.
[26] IAM. Asset management – an anatomy. Asset Management – an Anatomy; 2015.
[27] ISO. Water flow measurement in open channels using weirs and venturi flumes - Part 1: thin plate weirs. International Organization of Standards 1438/1-1980(E); 1980.
[28] Jongejan R, Stefess H, Roode N, ter Horst W, Maaskant B. The VNK2 project, a detailed, large scale quantitative flood risk analysis for the netherlands. In Icfm5; 2011.
[29] Kind J. Economically efficient flood protection standards for the Netherlands. J Flood Risk Manage 2014;7(2):103–17. Retrieved from, http://doi.wiley.com/10.1111/jfr3.12026.
[30] Kindsvater C, Carter R. Discharge characteristics of rectangular thin-plate weirs. Transactions, 24. American society of civil engineers; 1959. Paper no. 3001.
[31] Klerk WJ, Kanning W, Kok M, Wolfert R. Optimal planning of flood defence system reinforcements using a greedy search algorithm. Reliab Eng Syst Saf 2021;207:107344.

[32] Kok M, Jongejan R, Nieuwjaar M, Tanczos I. Fundamentals of flood protection. ISBN 978-90-8902-160-1. Ministry of Infrastructure and the Environment & Expertise Network for Flood Protection; 2017.
[33] Liu Q, Tang A, Huang D, Huang Z, Zhang B, Xu X. Total probabilistic measure for the potential risk of regional roads exposed to landslides. Reliab Eng Syst Saf 2022;228:108822.
[34] Manocha N, Babovic V. Development and valuation of adaptation pathways for storm water management infrastructure. Environ Sci Policy 2017;77:86–97.
[35] Mens MJP. Analyse van systeemrobuustheid (Tech. rep.). ISBN/EAN: 978-94-90070-55-7. Deltares; 2012.
[36] Ministerie van Infrastructuur en Milieu. (2016). Wet van 2 november 2016 tot wijziging van de Waterwet en enkele andere wetten (Waterwet). Retrieved from https://wetten.overheid.nl/BWBR0025458/2021-07-01.
[37] Mühlhofer E, Koks EE, Kropf CM, Sansavini G, Bresch DN. A generalized natural hazard risk modelling framework for infrastructure failure cascades. Reliab Eng Syst Saf 2023;234:109194.
[38] Pang Z, Li T, Pei H, Si X. A condition-based prognostic approach for age- and state-dependent partially observable nonlinear degrading system. Reliab Eng Syst Saf 2023;230:108854.
[39] Pathirana A, den Heijer F, Sayers P. Water infrastructure asset management is evolving. Infrastructures 2021;6(6).
[40] Roubos AA, Allaix DL, Schweckendiek T, Steenbergen RDJM, Jonkman SN. Time-dependent reliability analysis of serviceproven quay walls subject to corrosion-induced degradation. Reliab Eng Syst Saf Retriev 2020. https://doi.org/10.1016/j.ress.2020.107085.
[41] Ruiz-Tagle A, Lopez-Droguett E, Groth KM. A novel probabilistic approach to counterfactual reasoning in system safety. Reliab Eng Syst Saf 2022;228:108785.
[42] Samuels P, Klijn F, Dijkman J. An analysis of the current practice of policies on river flood risk management in different countries. Irrigat Drain 2006;55:141–50. Retrieved from, onlinelibrary.wiley.com/doi/10.1002/ird.257.
[43] Sayers P. Flood risk - Planning, design and management of flood defence infrastructure. ISBN 978-0-7277-5749-4. ICE Publishing; 2012.
[44] Sayers P. Strategic flood risk management: a systems-based approach (Doctoral dissertation. TU Delft, ISBN 978-90-73445-51-2); 2023. Retrieved from, https://ihedelftrepository.contentdm.oclc.org/digital/collection/phd1/id/62769.
[45] Sayers P, Galloway G, Penning-Rowsell E, Yuanyuan L, Fuxin S, Yiwei C, Guan Y. Strategic flood management: ten 'golden rules' to guide a sound approach. Int J River Basin Manag 2015. Retrieved from, https://www.tandfonline.com/action/journalInformation?journalCode=trbm20.
[46] Sayers P, Hall JW, Meadowcroft IC. Towards risk-based flood hazard management in the UK. In: Proceedings of the institution of civil engineers: civil engineering. 150; 2002. p. 36–42. SPECIAL ISSUE.
[47] Sayers P, Li Y, Galloway G, Penning-Rowsell E, Shen F, Wen K, Le Quesne T. Flood risk management: a strategic approach — asian development bank. asian development bank, manila; china general institute of water resources and hydropower planning and design, ministry of water resources. Beijing; UNESCO, Paris: WWF International, Gland Switzerland; 2013. Retrieved from, www.adb.org/publications/flood-risk-management-strategic-approach.
[48] Schultz M, Gouldby B, Simm J, Wibowo J. Beyond the factor of safety:developing fragility curves to characterize system reliability (Tech. rep.). Geotechnical and Structural Laboratory, ERDC; 2010. SR-10-1.
[49] Sharma N, Nocera F, Gardoni P. Classification and mathematical modeling of infrastructure interdependencies. Sustainable and Resilient Infrastructure; 2020.
[50] Slootjes N, Wagenaar D. Factsheets normering primaire waterkeringen (factsheets standardization primary flood defences) (Tech. rep.). ministerie van infrastructuur en milieu. DG Ruimte en Water, Directie Algemeen Waterbeleid en Veiligheid; 2016.
[51] Smale AJ. Werkwijzer bepaling hydraulische ontwerprandvoorwaarden, aanvulling OI2014, versie 5 (Hydra-NL 2.4.1) (Tech. rep.). Deltares; 2018.
[52] Smet K. Engineering options: a proactive planning approach for aging water resource infrastructure under uncertainty. Harvard University, Graduate School of Arts & Sciences; 2017.
[53] Steenbergen H, Lassing B, Vrouwenvelder A, Waarts PH. Reliability analysis of flood defence systems. Heron 2004;49(1):51–73.
[54] Toimil A, Losada IJ, Hinkel J, Nicholls RJ. Using quantitative dynamic adaptive policy pathways to manage climate change-induced coastal erosion. Climat Risk Manag 2021;33:100342.
[55] Van Der Meer JW, Ter Horst WLA, Van Velzen EH. Calculation of fragility curves for flood defence assets. Flood Risk Management: Research and Practice; 2009.
[56] Van Mierlo MC, Vrouwenvelder AC, Calle EO, Vrijling JK, Jonkman SN, De Bruijn KM, Weerts AH. Assessment of flood risk accounting for river system behaviour. Int J River Basin Manag 2010;5(2):93–104. Retrieved from, tandfonline.com/doi/abs/10.1080/15715124.2007.9635309.
[57] van Dantzig D. Economic Decision Problems for Flood Prevention. Econometrica 1956;24(3):276.
[58] van den Boomen M. Replacement optimization of ageing infrastructure under differential inflation. Technical University of Delft; 2020.
[59] van den Hurk B, Klein Tank A, Lenderink G, van Ulden A, van Oldenborgh G, Katsman C, Drijfhout S. KNMI climate change scenarios 2006 for the Netherlands (Tech. rep.). WR2006-01. KNMI; 2006.
[60] Vanmarcke EH. Matrix formulation of reliability analysis and reliability-based design. Comput Struct 1973;3(4):757–70.
[61] Vergouwe, R. (2014). De veiligheid van Nederland in kaart: eindrapportage VNK. Rijkswaterstaat, projectbureau VNK. Retrieved from repository.tudelft.nl/islandora/object/uuid{\%}3A52035faa-43ab-4dd0-a5b0-099119085356</bib>.
[62] Verheij H. Aanpassen van het bresgroeimodel in his-om (Tech. rep.). Delft: Q3299, WL—Delft Hydraulics; 2003.
[63] Vonk B, Klerk WJ, Fröhle P, Gersonius B, den Heijer F, Jordan P, Ashley R. Adaptive asset management for flood protection: the fair framework in action, 5. Infrastructures; 2020.
[64] Vorogushyn, S. (2008). Analysis of flood hazard under consideration of dike breaches (Doctoral dissertation, Potsdam). Retrieved from opus.kobv.de/ubp/volltexte/2009/2764/.
[65] Vorogushyn S, Merz B, Apel H. Development of dike fragility curves for piping and micro-instability breach mechanisms. Nat Hazard Earth Syst Sci 2009;9(4):1383–401.
[66] Wang J, Liu H, Lin T. Optimal rearrangement and preventive maintenance policies for heterogeneous balanced systems with three failure modes. Reliab Eng Syst Saf 2023;238:109429.
[67] Wojciechowska K, Pleijter G, Zethof M, Havinga FJ, Van Haaren DH, Ter Horst WLA. Application of fragility curves in operational flood risk assessment. Geotechnical safety and risk v; 2015. p. 528–34.
[68] Xiahou T, Zheng YX, Liu Y, Chen H. Reliability modeling of modular k-out-of-n systems with functional dependency: a case study of radar transmitter systems. Reliab Eng Syst Saf 2023;233:109120.
[69] Yang DY, Frangopol DM. Risk-based portfolio management of civil infrastructure assets under deep uncertainties associated with climate change: a robust optimisation approach. Struct Infrastruct Eng 2020;16(4).
[70] Young K, Hall JW. Introducing system interdependency into infrastructure appraisal: from projects to portfolios to pathways. Infrastructure Complexity 2015;2(2):1–18. Retrieved from, infrastructure-complexity.springeropen.com/articles/10.1186/s40551-015-0005-8.
[71] Zhuang L, Xu A, Wang XL. A prognostic driven predictive maintenance framework based on Bayesian deep learning. Reliab Eng Syst Saf 2023;234:109181.